

Fatty Acids Identified in the Burmese Python Promote Beneficial
Cardiac Growth

Cecilia A. Riquelme et al.

Deposited 2023-09-27

Citation of published version:

Riquelme, C. A., Magida, J. A., Harrison, B. C., Wall, C. E., Marr, T. G., Secor, S. M., & Leinwand, L. A. (2011). Fatty Acids Identified in the Burmese Python Promote Beneficial Cardiac Growth. In *Science* (Vol. 334, Issue 6055, pp. 528–531). American Association for the Advancement of Science (AAAS).
<https://doi.org/10.1126/science.1210558>



Published in final edited form as:

Science. 2011 October 28; 334(6055): 528–531. doi:10.1126/science.1210558.

Fatty Acids Identified in the Burmese Python Promote Beneficial Cardiac Growth

Cecilia A. Riquelme¹, Jason A. Magida¹, Brooke C. Harrison¹, Christopher E. Wall¹, Thomas G. Marr², Stephen M. Secor³, and Leslie A. Leinwand¹

¹Department of Molecular, Cellular, and Developmental Biology, University of Colorado at Boulder, Boulder, CO 80309

²Hiberna Corporation, Boulder, CO 80302

³Department of Biological Sciences, University of Alabama, Tuscaloosa, AL, 35487

Abstract

Burmese pythons display a dramatic increase in heart mass after a large meal. We investigated the molecular mechanisms of this physiological heart growth, with the goal of applying this knowledge to the mammalian heart. We found that heart growth in pythons is characterized by myocyte hypertrophy in the absence of cell proliferation and by activation of PI3K/Akt/mTor signaling pathways. Despite high levels of circulating lipids, the postprandial python heart does not accumulate triglycerides or fatty acids. Instead, there is robust activation of pathways of fatty acid transport and oxidation combined with increased expression and activity of the cardioprotective enzyme, superoxide dismutase. Finally, we identified a combination of fatty acids in python plasma that promotes physiological heart growth when injected into either pythons or mice.

The heart is a highly adaptable organ that demonstrates remarkable cellular remodeling in the face of both pathological and physiological stimuli. Insults such as myocardial infarction, chronic hypertension, or genetic mutations affecting sarcomeric or calcium handling proteins activate pathological hypertrophic signaling cascades including those mediated by the α 1-adrenergic and endothelin receptors. This ultimately results in increased cell size, enhanced sarcomere assembly, and activation of a 'fetal' gene program, with increased expression of β -myosin heavy chain (β -MyHC), α -skeletal actin, and the atrial and brain natriuretic peptides (ANP and BNP, respectively) combined with reduced expression of α -MyHC and the sarcoplasmic reticulum Ca^{2+} ATPase-2 (SERCA2)(1–3). Importantly, pathological insults also typically result in a switch in metabolic substrate utilization from lipidoxidation to glucose utilization and increased apoptosis and fibrosis(1, 3). Conversely, physiological cardiac hypertrophy resulting from post-natal growth, pregnancy, or exercise is primarily mediated by insulin-like growth factor-1 (IGF-1) signaling and activation of PI3K/Akt signaling in the absence of fetal gene program activation(4, 5). Unlike pathological cardiac hypertrophy, this adaptive hypertrophy does not appear to be detrimental to cardiac function. In fact, exercise-induced physiological cardiac growth protects the heart against pathological stimuli such as pressure overload(6).

The infrequently feeding Burmese python (*Python molurus*) has been described as a model of extreme metabolic regulation in which many organs, including the heart increase in mass after a large meal (7, 8). While most mammalian models of physiological hypertrophy typically demonstrate modest hypertrophy (~10–20%) after weeks of stimulation, the python heart grows in mass by 40% within 48–72 hours after consumption of a large meal(7–9). This remarkable cardiac hypertrophy is accompanied by increased cardiac output and appears to be an adaptive response to support the large (~44-fold) increase in postprandial

metabolic rate accompanied by increased systemic nutrient transport and widespread organ growth(7–12). While there has been some initial description of the cardiac hypertrophy observed in this model, the underlying molecular and cellular mechanisms have yet to be determined(7, 8, 13). Given that pathological cardiac hypertrophy is a leading predictor of mortality, we sought to understand the cellular and molecular components of this rapid and dramatic cardiac enlargement and potentially identify new mechanisms regulating physiological cardiac growth.

Similar to previous reports, we observed a progressive increase in heart size over the post-feeding time period (Figures 1A and S1A), with a maximum increase seen at 3 days post-feeding (DPF)(Figure S1A)(14). As in mammals, cardiac growth in the python appeared to be hypertrophic rather than hyperplastic, as there was no sign of cardiac BrdU incorporation in the postprandial heart (Figure 1B). While the cellular architecture of the python ventricle did not allow for reliable quantification of myocyte size (Figure S1B), we observed a significant reduction in the number of nuclei per field in the 3 DPF ventricle, providing indirect evidence of cellular hypertrophy in the absence of cell division (Figure 1C). Interestingly, the fasted python myocardium was significantly more fibrotic than a normal mammalian heart (~18% vs. ~1–2%)(15)and the degree of fibrosis remained relatively unchanged throughout digestion of the meal (Figure S1C). The postprandial python heart demonstrated an atypical pattern of gene expression, with increased expression of both SERCA2 and α -skeletal actin mRNA, as well as a progressive increase in both MYH7 (β -MyHC) and a less-characterized striated muscle myosin heavy chain gene, MYH15 which is also the predominant MyHC isoform expressed in the chicken heart (Figure S2)(16). Western blot analyses revealed increased phosphorylation of AMPK, Akt, GSK3 β , and mTOR during the postprandial period (Figures 1D and S3), indicating robust activation of protein synthetic pathways in the postprandial python heart.

Consistent with published observations(7), we observed a large (52-fold) increase in plasma triglycerides and a 3-fold increase in free fatty acids (FFAs) at 1DPF (Figure 2A). In most mammals, comparable plasma triglyceride concentrations would result in pathogenic lipid deposition in non-adipose tissues such as the heart(17). In the python heart, however, thin layer chromatography (TLC) and Oil red-Oanalysis did not reveal any evidence of lipid accumulation during the postprandial period (Figures 2B and S4A). We also found no change in cardiac VLDLR transcript levels, suggesting that utilization of triglyceride-rich lipoprotein particles is not altered post-feeding (Figure S4B). Despite this lack of cardiac lipid accumulation, expression of the fatty acid transporter CD36 was *increased* 13-fold at 1 DPF (Figure 2C). mRNA levels of both muscle-type fatty acid binding protein (mFABP)and carnitine palmitoyl1B transferase (CPT1B)were significantly increased post-feeding (Figure 2C) as were mitochondrial cytochrome oxidase (COX2) expression and nicotinamide adenine dinucleotide tetrazolium reductase (NADH-TR) staining (Figure 2B). We also observed increased expression of several oxidative genes at 1 and 3 DPF, including medium-chain acyl-CoA dehydrogenase (MCAD), enoyl-CoA hydratase (ECHD), and β -ketoacyl-CoA thiolase (ACAA2) (Figure 2C). Together, these data suggest that there is increased oxidative capacity in the postprandial python heart. Importantly, these apparent alterations in mitochondrial electron transport chain flux were coupled with a significant increase in both expression and activity of the cardioprotective free radical scavenging enzyme SOD2 (Figure 2D)(18) and we found no evidence of increased reactive oxygen species in the postprandial heart (Figure S5).

To investigate the possibility that the systemic changes observed in the python were due to circulating factors, we tested the effect of python plasma on neonatal rat ventricular myocytes (NRVMs) in culture. In fact, treatment of NRVMs with fed plasma significantly increased cell size and α -actinin organization (Figures 3A and S6). Interestingly, the degree

of NRVM growth induced by the specific postprandial plasma time points mimicked the time profile of *in vivo* python heart growth (Figures 3A and S1A), suggesting that the plasma concentrations of the hypertrophic factors varied throughout digestion. While cells treated with the α -adrenergic agonist phenylephrine clearly demonstrated robust activation of pathological patterns of gene expression, we found no such gene activation in cells treated with python plasma (Figure 3B). We also determined that treatment of NRVMs with fed python plasma resulted in increased IGF-1 mRNA expression and enhanced phosphorylation of mTor and p70S6K (Figure S7). Intriguingly, fasted or fed python plasma significantly *repressed* NFAT activity, a canonical indicator of pathological hypertrophic signaling, in NRVMs (Figure 3C). Finally, treatment of NRVMs with fed python plasma significantly increased the expression of key lipid handling (mFABP) and metabolism genes (CPT1B, MCAD, and ACAA2) in a manner similar to that observed in the fed python heart (Figure S8).

Given the dramatic alterations seen in postprandial plasma lipid content and the evidence that heat treatment and protease K digestion were ineffective in eliminating the pro-hypertrophic effects of the fed python plasma (Figure S9), we focused our attention on lipid species as candidate pro-hypertrophic factors. In support of this, pretreatment of NRVMs with an irreversible inhibitor of CD36 (sulfosuccinimidyl-oleate [SSO] (19)) completely blocked the pro-hypertrophic effect of fed plasma (Figure S10). We then analyzed fasted and post-fed python plasma by gas chromatography (GC) and observed a highly complex composition of circulating fatty acids with distinct patterns of abundance over the course of digestion (Figure S11). Based on these data, identified 5 candidate fatty acids for further analysis (Figure S12) and determined that supplementing fasted python plasma with the 1 DPF molar ratio of C14:0 (myristic acid), C16:0 (palmitic acid), and C16:1n7 (palmitoleic acid) effectively recapitulated the increase in NRVM cell diameter seen with 1 DPF plasma (Figure 3D). Similar to the effects seen with fed python plasma, treatment of NRVMs with this fatty acid mixture resulted in robust up-regulation of CD36, mFABP, CPT1, MCAD, and ACAA2 mRNA expression (Figure S8). Despite the established, pro-apoptotic properties of palmitic acid in cardiomyocytes (20–22), we did not find any evidence of apoptosis in NRVMs cultured in the presence of python plasma or the fatty acid combination (Figure S13). These data suggest that palmitoleic acid may protect cardiomyocytes from apoptosis in the presence of palmitic acid. While the mechanism for this protection is unknown, it is possible that the presence of palmitoleic acid combined with increased oxidative capacity and free-radical scavenging capacity may act to reduce the generation of toxic, pro-apoptotic intermediates such as ceramide and reactive oxygen species, and enhance the activity of cardioprotective pathways such as triglyceride biosynthesis and β -oxidation (21–23).

To investigate the ability of these fatty acids to trigger cardiac growth *in vivo*, we infused fasted pythons with the same mixture of myristic, palmitic, and palmitoleic acid and determined that this lipid infusion was as effective at stimulating cardiac growth as either feeding itself or infusion of plasma from a fed snake (Figure 4A). Finally, we administered the fatty acid mixture to mice over a 7-day period and observed a significant increase in left ventricular mass (Figure 4B), increased cardiomyocyte cross-sectional area (Figure 4B), no activation of the pathological fetal gene program (Figure 4C), and no evidence of alterations in cardiac fibrosis or lipid deposition (Figure S14). Intriguingly, the growth-inducing effects of the fatty acids appeared to be cardiac-specific, as there were no observed alterations in either liver or skeletal muscle mass (Figure S15A). As a control, we also administered a mixture of oleic (C18:1), linoleic (C18:2), and arachidonic (C20:4) acid in the molar ratio observed in the 1 DPF python and saw no evidence of cardiac hypertrophy (Figure S15B), indicating that the pro-hypertrophic effects are specific to the mixture of myristic, palmitic, and palmitoleic acid. Interestingly, palmitoleic acid has recently been characterized as a

lipokine that can modulate systemic insulin sensitivity (24). Additionally, fatty acid ethanolamides (FAEs) have been described as potent regulators of energy intake, and levels of the palmitoleic acid ethanolamide, palmitoleylethanolamide (and other FAEs), are dramatically increased in the fed python gastrointestinal tract (25). Together, these data and our data suggest multiple roles for palmitoleic acid and its metabolites in the regulation of insulin sensitivity, organ size, cardiac metabolism, and energy balance (24–26).

Overall, our results indicate that postprandial cardiac growth in the python is characterized by cellular hypertrophy in the absence of hyperplasia and activation of PI3K/Akt/mTOR signaling pathways. Despite elevations in circulating triglycerides and increased fatty acid transport, the python heart appears to be protected from lipid deposition through increased oxidative capacity and induction of free radical scavenging activity. Finally, we demonstrate that a combination of fatty acids, identified in postprandial python plasma, promotes physiological hypertrophy in mammalian cardiomyocytes. Given that activation of adaptive, physiological hypertrophic processes can provide functional benefit in the context of a cardiac disease state, our data indicate that fatty acid supplementation may provide a new mechanism for modulating cardiac gene expression and function in mammals, and that such interventions could augment cardiac performance in the context of human disease.

Supplementary Material

Refer to Web version on PubMed Central for supplementary material.

Acknowledgments

Supported by NIH grant HL050560 (L.A.L.), NSF grant IOS-0466139 (S.M.S.), University of Colorado Technology Transfer Office/State of Colorado grant OCG4999B (L.A.L. and T.G.M.), Hiberna Corporation (T.G.M. and S.M.S.), American Heart Association fellowship 0725732Z (C.A.R.), and NIH grant 5K01AR055676 (B.C.H.). L.A.L., T.G.M., and B.C.H. are on the scientific advisory board of, and are shareholders in, Hiberna Corporation, a company that is developing drugs based on natural models of extreme metabolic regulation. C.A.R. is a shareholder in Hiberna Corporation. The authors (L.A.L., C.A.R., J.A.M., B.C.H.) and the University of Colorado have filed a patent relating to methods and compositions for inducing physiological cardiac hypertrophy. We thank S. Cozza and T. Gleason for their technical assistance.

References and Notes

1. Frey N, Olson EN. Cardiac hypertrophy: the good, the bad, and the ugly. *Annu Rev Physiol.* 2003; 65:45. [PubMed: 12524460]
2. Calderone A, Takahashi N, Izzo NJ Jr, Thaik CM, Colucci WS. Pressure- and volume-induced left ventricular hypertrophies are associated with distinct myocyte phenotypes and differential induction of peptide growth factor mRNAs. *Circulation.* 1995 Nov 1.92:2385. [PubMed: 7586335]
3. Olson EN. A decade of discoveries in cardiac biology. *Nat Med.* 2004 May.10:467. [PubMed: 15122248]
4. Harrison BC, et al. The CRM1 nuclear export receptor controls pathological cardiac gene expression. *Mol Cell Biol.* 2004 Dec.24:10636. [PubMed: 15572669]
5. Fagard R. Athlete's heart. *Circulation.* 2001 Feb 13.103
6. Konhilas JP, et al. Exercise can prevent and reverse the severity of hypertrophic cardiomyopathy. *Circ Res.* 2006 Mar 3.98:540. [PubMed: 16439687]
7. Secor SM, Diamond J. A vertebrate model of extreme physiological regulation. *Nature.* 1998 Oct 15.395:659. [PubMed: 9790187]
8. Andersen JB, Rourke BC, Caiozzo VJ, Bennett AF, Hicks JW. Physiology: postprandial cardiac hypertrophy in pythons. *Nature.* 2005 Mar 3.434:37. [PubMed: 15744290]
9. Secor SM, Diamond J. Adaptive responses to feeding in Burmese pythons: pay before pumping. *J Exp Biol.* 1995 Jun.98:1313.

10. Secor SM, Diamond J. Determinants of the postfeeding metabolic response of Burmese pythons, *Python molurus*. *Physiol Zool*. 1997 Mar-Apr;70:202. [PubMed: 9231393]
11. Secor SM. Digestive physiology of the Burmese python: broad regulation of integrated performance. *J Exp Biol*. 2008 Dec.211:3767. [PubMed: 19043049]
12. Secor SM, White SE. Prioritizing blood flow: cardiovascular performance in response to the competing demands of locomotion and digestion for the Burmese python, *Python molurus*. *J Exp Biol*. 2010 Jan 1.213:78. [PubMed: 20008365]
13. Wall CE, et al. Whole transcriptome analysis of the fasting and fed Burmese python heart: insights into extreme physiological cardiac adaptation. *Physiol Genomics*. 2011 Jan 1.46:69. [PubMed: 21045117]
14. Materials and methods are available as supporting material on Science Online.
15. Diwan A, et al. Nix-mediated apoptosis links myocardial fibrosis, cardiac remodeling, and hypertrophy decompensation. *Circulation*. 2008 Jan 22.117:396. [PubMed: 18178777]
16. Rossi AC, Mammucari C, Argentini C, Reggiani C, Schiaffino S. Two novel/ancient myosins in mammalian skeletal muscles: MYH14/7b and MYH15 are expressed in extraocular muscles and muscle spindles. *J Physiol*. 2010 Jan 15.588:353. [PubMed: 19948655]
17. Khan RS, Drosatos K, Goldberg IJ. Creating and curing fatty hearts. *Curr Opin Clin Nutr Metab Care*. 2010 Mar.13:145. [PubMed: 20010095]
18. Shimizu T, Nojiri H, Kawakami S, Uchiyama S, Shirasawa T. Model mice for tissue-specific deletion of the manganese superoxide dismutase gene. *Geriatr Gerontol Int*. 2010 Jul.10(Suppl 1):S70. [PubMed: 20590844]
19. Coort SL, et al. Sulfo-N-succinimidyl esters of long chain fatty acids specifically inhibit fatty acid translocase (FAT/CD36)-mediated cellular fatty acid uptake. *Mol Cell Biochem*. 2002 Oct. 239:213. [PubMed: 12479588]
20. Sparagna GC, Hickson-Bick DL, Buja LM, McMillin JB. Fatty acid-induced apoptosis in neonatal cardiomyocytes: redox signaling. *Antioxid Redox Signal*. 2001 Feb.3:71. [PubMed: 11291600]
21. Miller TA, et al. Oleate prevents palmitate-induced cytotoxic stress in cardiac myocytes. *Biochem Biophys Res Commun*. 2005 Oct 14.336:309. [PubMed: 16126172]
22. de Vries JE, et al. Saturated but not mono-unsaturated fatty acids induce apoptotic cell death in neonatal rat ventricular myocytes. *J Lipid Res*. 1997 Jul.38:1384. [PubMed: 9254064]
23. Hickson-Bick DL, Buja LM, McMillin JB. Palmitate-mediated alterations in the fatty acid metabolism of rat neonatal cardiac myocytes. *J Mol Cell Cardiol*. 2000 Mar.32:511. [PubMed: 10731449]
24. Cao H, et al. Identification of a lipokine, a lipid hormone linking adipose tissue to systemic metabolism. *Cell*. 2008 Sep 19.134:933. [PubMed: 18805087]
25. Astarita G, et al. Postprandial increase of oleoylethanolamide mobilization in small intestine of the Burmese python (*Python molurus*). *Am J Physiol Regul Integr Comp Physiol*. 2006 May. 290:R1407. [PubMed: 16373434]
26. van der Lee KA, et al. Long-chain fatty acid-induced changes in gene expression in neonatal cardiac myocytes. *J Lipid Res*. 2000 Jan.41:41. [PubMed: 10627500]
27. Helmstetter C, et al. Functional changes with feeding in the gastro-intestinal epithelia of the Burmese python (*Python molurus*). *Zoolog Sci*. 2009 Sep.26:632. [PubMed: 19799514]
28. Harrison BC, Bell ML, Allen DL, Byrnes WC, Leinwand LA. Skeletal muscle adaptations in response to voluntary wheel running in myosin heavy chain null mice. *J Appl Physiol*. 2002 Jan. 92:313. [PubMed: 11744674]
29. Waspe LE, Ordahl CP, Simpson PC. The cardiac beta-myosin heavy chain isogene is induced selectively in alpha 1-adrenergic receptor-stimulated hypertrophy of cultured rat heart myocytes. *J Clin Invest*. 1990 Apr.85:1206. [PubMed: 2156896]
30. Harmon CM, Luce P, Beth AH, Abumrad NA. Labeling of adipocyte membranes by sulfo-N-succinimidyl derivatives of long-chain fatty acids: inhibition of fatty acid transport. *J Membr Biol*. 1991 May.121:261. [PubMed: 1865490]
31. MacMillan-Crow LA, Crow JP, Kerby JD, Beckman JS, Thompson JA. Nitration and inactivation of manganese superoxide dismutase in chronic rejection of human renal allografts. *Proc Natl Acad Sci U S A*. 1996 Oct 15.93:11853. [PubMed: 8876227]

32. Folch J, Lees M, Sloane Stanley GH. A simple method for the isolation and purification of total lipides from animal tissues. *J Biol Chem.* 1957 May;226:497. [PubMed: 13428781]

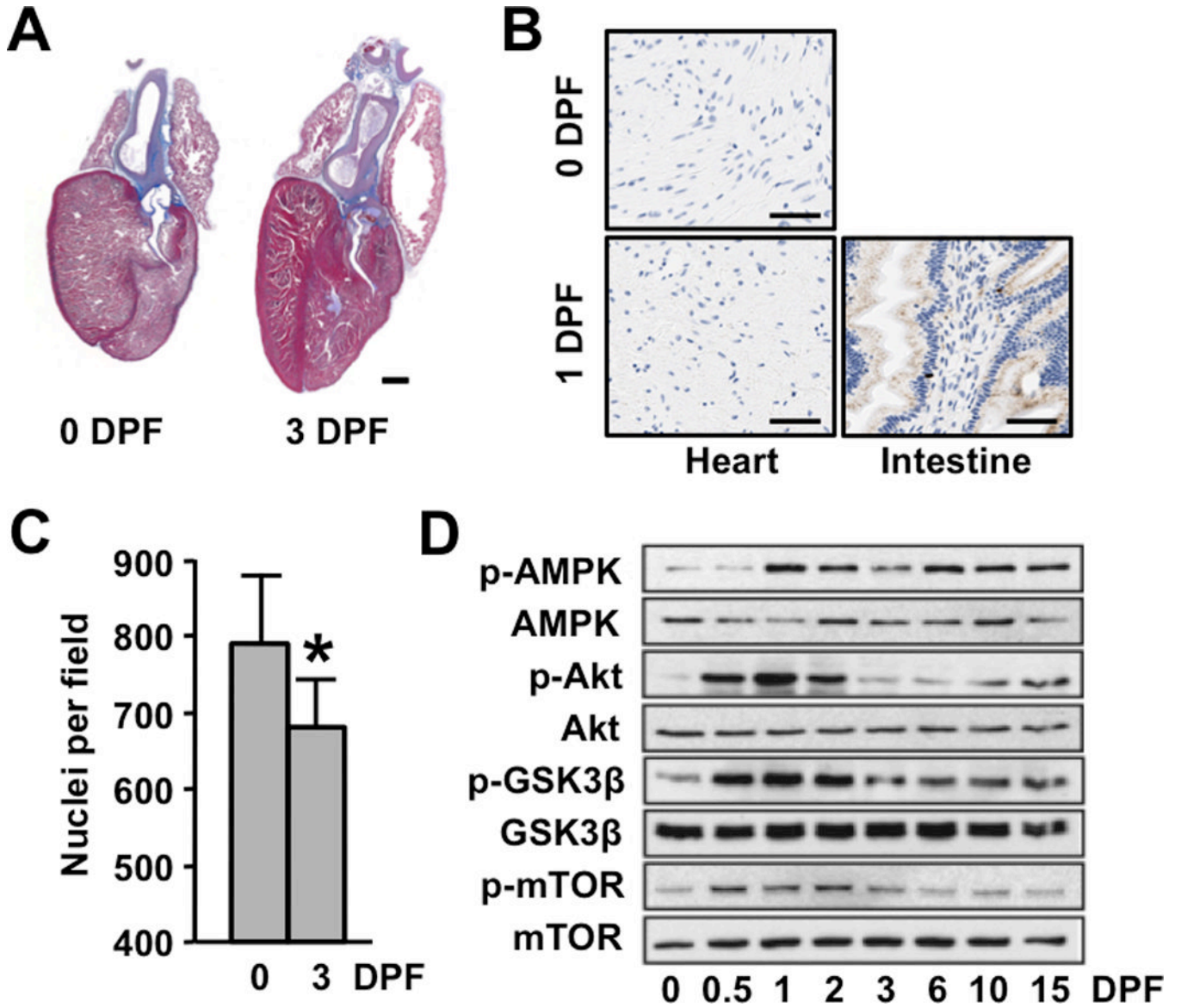


Figure 1. Postprandial cardiac growth in the python is characterized by cellular hypertrophy and activation of protein synthesis pathways. (A) Masson trichrome–stained python hearts depicting pronounced postprandial cardiac hypertrophy. Scale bar = 2 mm (B) BrdU-staining of 0 and 3 DPF python hearts shows no evidence of postprandial cellular proliferation (python small intestine is included as a positive control [brown nuclear staining]) Scale bar = 50 μ m (C) The number of nuclei per field is reduced post-feeding. (D) Immunoblot analysis reveals increased phosphorylation of AMPK, Akt, GSK3 β , and mTor in the postprandial python heart. Error bars represent \pm SE; n=4 per condition; *p<0.05 versus 0 DPF.

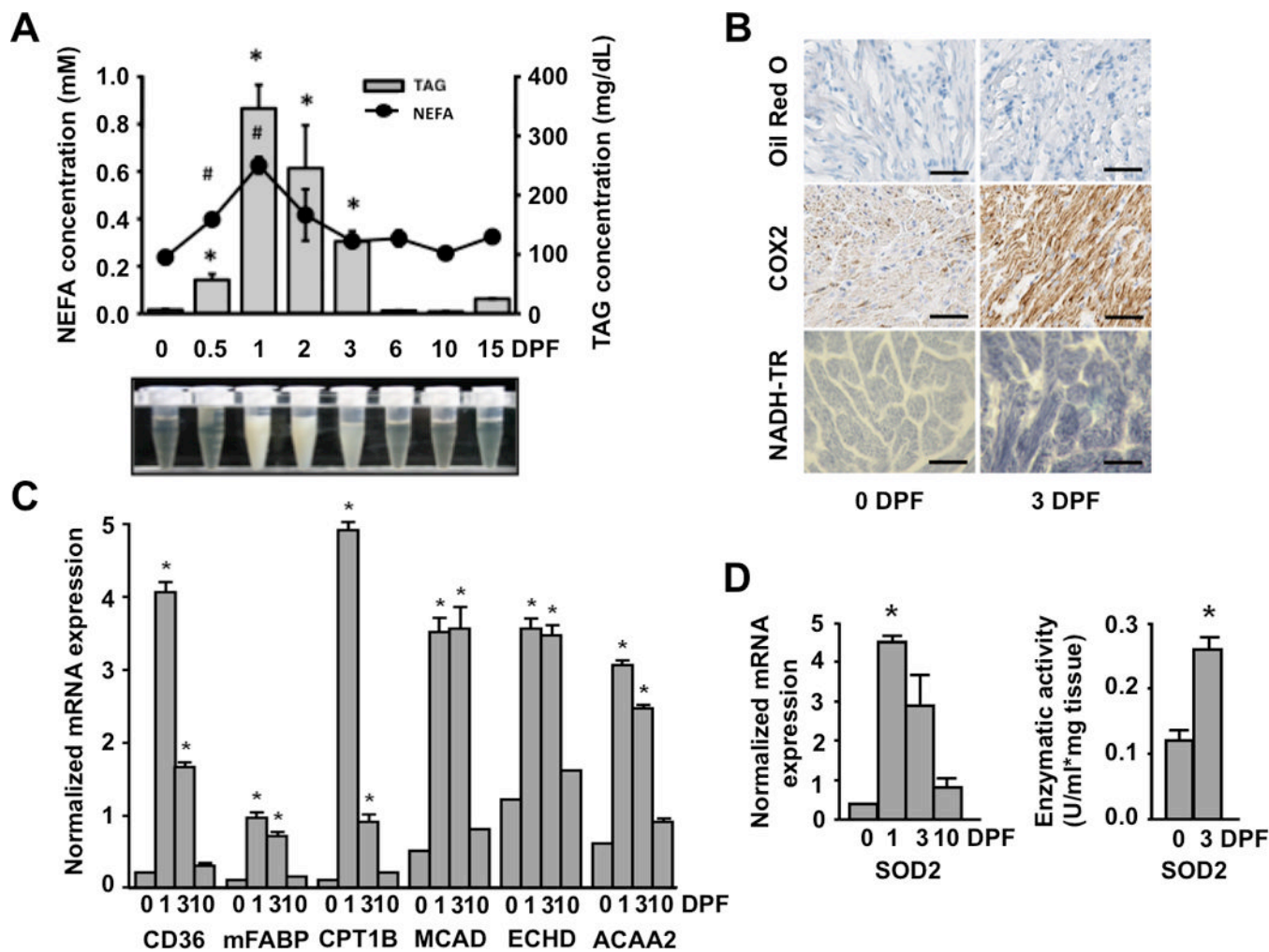


Figure 2.

The postprandial python heart has increased expression of fatty acid transport, handling, and oxidation genes along with enhanced free radical scavenging capacity. (A) Plasma fatty acid (FA) and triacylglyceride (TAG) content is significantly increased post-feeding (B) Oil Red-O staining reveals no cardiac accumulation of neutral lipids at 3 days after feeding. Mitochondrial staining is increased in the post-fed python heart as determined by cytochrome c oxidase II (COX2) immunostaining and NADH-tetrazolium reductase (NADH-TR) histochemistry. Scale bar = 50 μ m. (C) There is increased mRNA expression of fatty acid transport protein (CD36), muscle-type fatty acid binding protein (mFABP), carnitine palmitoyltransferase (CPT1B), and the β -oxidation genes medium chain acyl-CoA dehydrogenase (MCAD), peroxisomal enoyl-CoA hydratase (ECHD) and acetyl-CoA acyltransferase 2 (ACAA2) post-feeding. (D) The mRNA expression and activity of mitochondrial superoxide dismutase 2 (SOD2) is increased post-feeding. Error bars represent \pm SE; n=4 per condition; * and # p<0.05 versus 0 DPF.

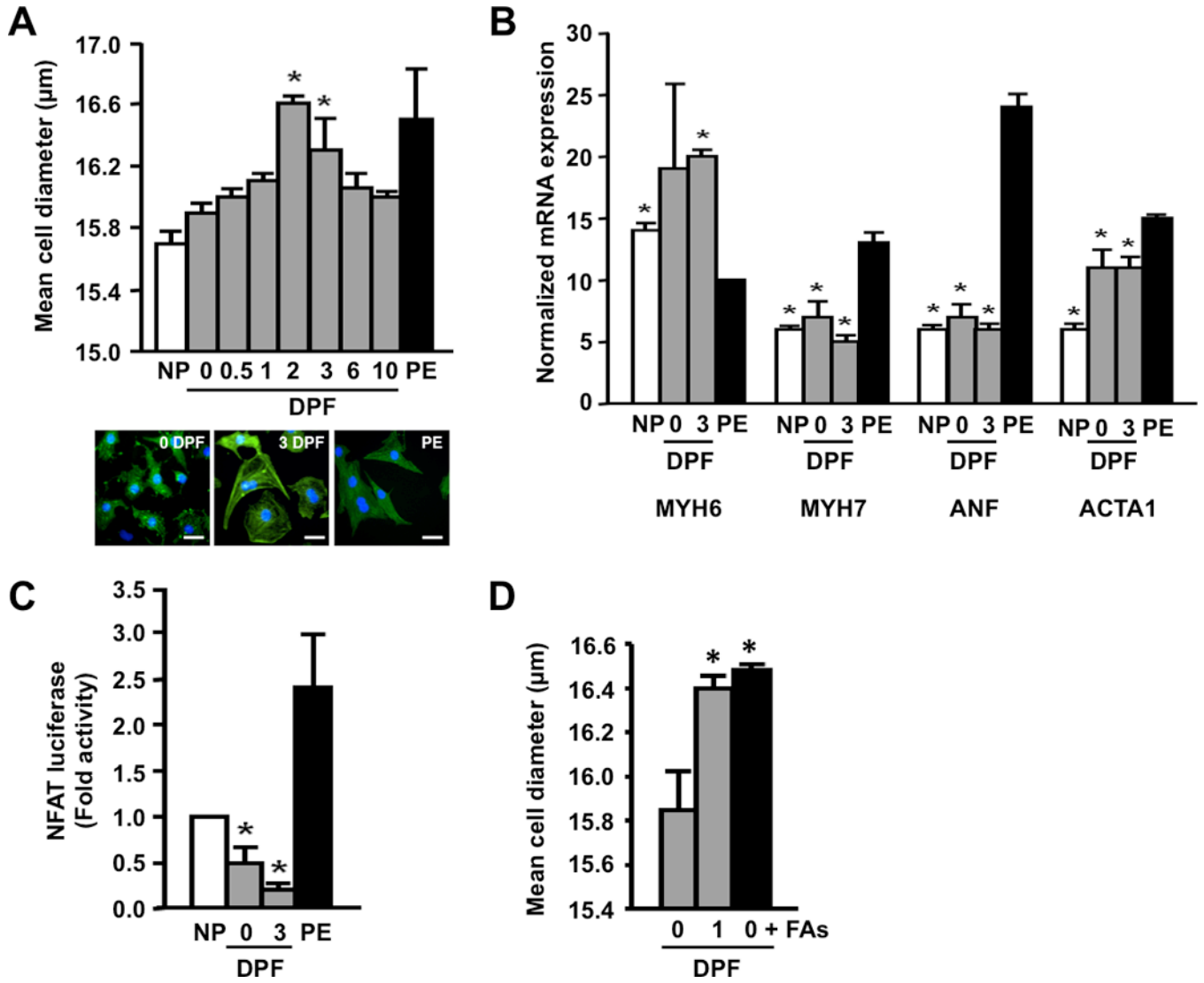


Figure 3. Postprandial python plasma induces cardiomyocyte growth in vitro. (A) Fed python plasma induces cellular hypertrophy in neonatal rat cardiac myocytes (NRVMs). Scale bar = 10 µm. (B) Python plasma does not induce the mRNA expression of known cardiac stress markers in NRVMs. PE, phenylephrine (included as a positive control); ANF, atrial natriuretic factor; MYH6, α-myosin heavy chain; MYH7, β-myosin heavy chain; ACTA1, α-skeletal actin. (C) Pathological NFAT signaling is repressed by python plasma. (D) Supplementing fasted python plasma with C14:0, C16:0, and C16:1n7 (0 DPF + FAs) results in cellular hypertrophy comparable to that seen with 1 DPF plasma. Error bars represent ±SE; n=3 per condition; *p<0.05 versus 0 DPF (A and D); *p<0.05 versus PE (B); *p<0.05 versus no plasma (NP, C).

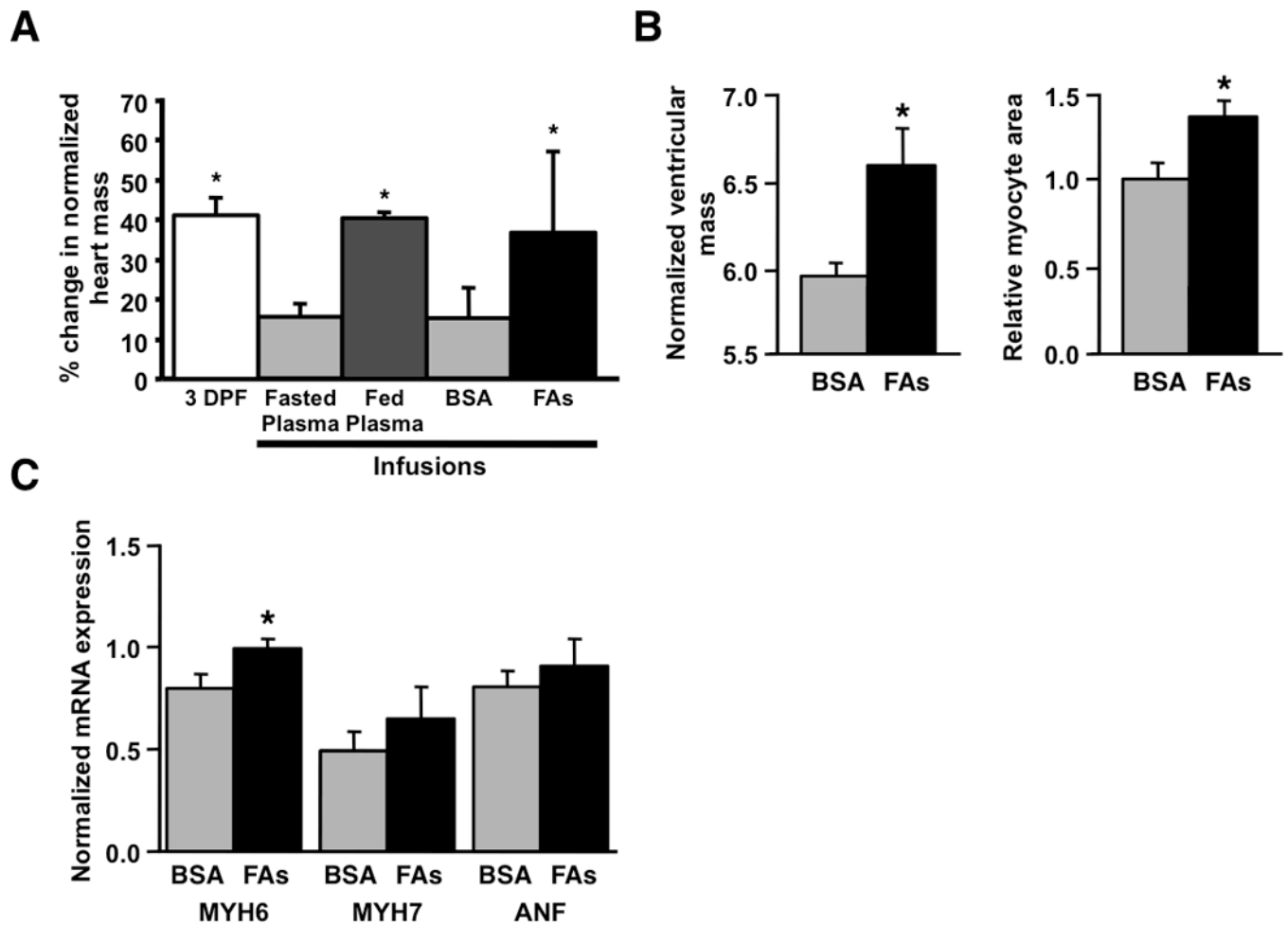


Figure 4.

Postprandial python plasma fatty acids induce cardiac growth in vivo. (A) Infusing fasted pythons with fed plasma or C14:0, C16:0, and C16:1n7 (FAs) results in increased heart mass (heart weight/body weight) comparable to that seen with ingestion of a rodent meal (3 DPF). (B) Seven day infusion of FAs in mice results in increased left ventricular mass (left ventricular mass/tibia length) and increased relative myocyte cross-sectional area. (C) FA infusion in mice results in increased MYH6 (α -myosin heavy chain) mRNA expression with no change in MYH7 (β -myosin heavy chain) or atrial natriuretic factor (ANF). Error bars represent \pm SE; n=3 (A) or 6 (B and C) per condition; *p<0.05 versus fasted python (A); *p<0.05 versus BSA (B and C).